

Numerical Simulation as Laboratory Liquefaction Test Comparison for Geological Hazard Countermeasure: A Preliminary Study

Arifan Jaya Syahbana^{1*}, Yelvi Yelvi², Adrin Tohari¹, and Prastika Wahid Santoso³

¹Researcher Center for Geological Disaster, National Research and Innovation Agency (BRIN), Jl. Sangkuriang No.1, Bandung 40135, Indonesia.

²Civil Engineering Department, State Polytechnic of Jakarta (PNJ), Jakarta 16425, Indonesia.

³Civil Engineering Department, Brawijaya University, Malang 65145, Indonesia.

Abstract. Liquefaction is a secondary hazard due to earthquakes, which is one of the geological hazards. The impairment caused can damage infrastructure on a wide scale and even cause casualties. Several phenomenal liquefaction events have been recorded throughout the world, and one of the most phenomenal is the flow liquefaction incident in Palu, Sulawesi, Indonesia, in 2018. Research on liquefaction is still ongoing today. In this study, numerical simulations will be carried out as a comparison for laboratory liquefaction tests, which aim to understand the flow liquefaction mechanism better. Laboratory modeling is presented carefully in numerical modeling, namely by creating three (3) variations in sand density layers in a box with dimensions of 120 cm x 60 cm x 40 cm. The simulation uses the assumption that the soil is perfectly saturated by placing the groundwater level at an elevation of 0 cm. The acceleration applied to the box is varied in the range of 0.3 – 0.6g. Simulation shows that deformation increases with the bigger magnitude and Peak Ground Acceleration (PGA), while the duration is not too sensitive to the results. On the other hand, the area liquefied is affected by the duration, magnitude, and PGA value.

1 Introduction

Liquefaction is a phenomenon of soil liquefaction that commonly occurs in locations where soil deposits are saturated sand, not dense and with relatively uniform gradations due to the propagation of seismic waves from earthquakes, thereby increasing pore water pressure. This phenomenon causes the soil to lose effective shear stress and the effect is the loss of the soil's bearing capacity. The extraordinary liquefaction event in the last decade was the Palu earthquake in 2018. This earthquake event resulted in liquefaction which damaged infrastructure and buildings in very large proportions.

Liquefaction in the form of mud flows left severe damage to most of the land on gentle slopes in Palu City within a distance of about 1 km [1–4]. Flow liquefaction covers the Balaroa, Petobo, and Jono Oge areas which are strongly influenced by the presence of alluvial

* Corresponding author: arif030@brin.go.id

soil deposits and shallow groundwater levels before the earthquake shock. Liquefaction events in Balaroa can be confirmed using semi-empirical analysis and a vulnerability index approach from microtremor surveys [5,6]. In addition, researchers also created a numerical model of the geotechnical effects of differences in seismic parameters [7]. This research was carried out by linking wave characteristics, land site classification, and evidence of liquefaction during the 2018 earthquake. Liquefaction can be triggered even on very gentle slopes with a slope of 2% - 3%.

Based on the field investigations that have been carried out, further laboratory scale investigations need to be carried out to clarify the liquefaction mechanism. Several previous studies conducted a series of shaking table tests on lateral soil flow due to liquefaction during an earthquake [8,9]. Based on the test results, the influence of slope, input movement, and thickness of the liquefaction layer on soil flow is investigated, and the fundamental characteristics of soil lateral flow induced by soil liquefaction are elucidated experimentally. Furthermore, some researchers investigated the liquefaction layer thickness factor based on the principle of minimum potential energy to predict permanent lateral displacement applied to real cases from shaking table tests and field case studies on past earthquakes [10,11]. Researcher [12] conducted a series of 1-g scale vibrating table model tests carried out on lateral flow on sand slopes experiencing high excess pore water pressure. Very low-density model sand deposits are prepared to induce lateral flow of varying degrees, with either sustained vibrations or short-impact vibrations. By changing the test conditions, the effects of vibration intensity, base excitation frequency, slope gradient, and sand density were investigated.

Based on the information above, this research carried out a comparative numerical analysis to clarify the liquefaction laboratory tests. This activity is important as an initial reference in studying the liquefaction phenomenon.

2 Method

Dynamic modeling uses the PLAXIS program to model a soil layer with dynamic loads in the form of earthquake loads which are represented by displacement in the bedrock of 1 cm. This displacement is a function of the earthquake acceleration spectrum with a certain PGA value adjusted to the existing site class (PGA MCER function). The spectrum function in the form of time history can be selected based on the earthquake mechanism to be simulated. After the soil layer is given a dynamic load, the total pore water pressure can be obtained. The soil mechanical properties used as parameters in PLAXIS modeling include soil specific gravity (γ), saturated specific gravity (γ_{sat}), permeability (k), Young's modulus (E), and internal friction angle (ϕ). Next are the test points. Analyzed at each specific depth that has the potential to experience liquefaction. The formula equation used is as follows [13–15].

$$\begin{aligned}\Delta p &= K_u \Delta \varepsilon_v \\ \Delta p' &= (1 - B) \Delta p = K' \Delta \varepsilon_v \\ \Delta p_w &= B \Delta p = \frac{K'}{n} \Delta \varepsilon_v\end{aligned}\quad (1)$$

where:

| | |
|--------------|---------------------------------|
| Δp | = total pore water pressure |
| $\Delta p'$ | = effective pore water pressure |
| Δp_w | = excess pore water pressure |
| K_u | = undrained Bulk Modulus |
| K' | = Bulk Modulus |
| n | = porosity |

$\Delta\varepsilon_v$ = volumetric strain increment
 B = Skempton factor

2.1 Model simulation

Simulation done with below dimension as depicted in Fig.1. Model presented with three (3) layer sand with different density. Slope also created to simulated geologic condition in Palu.

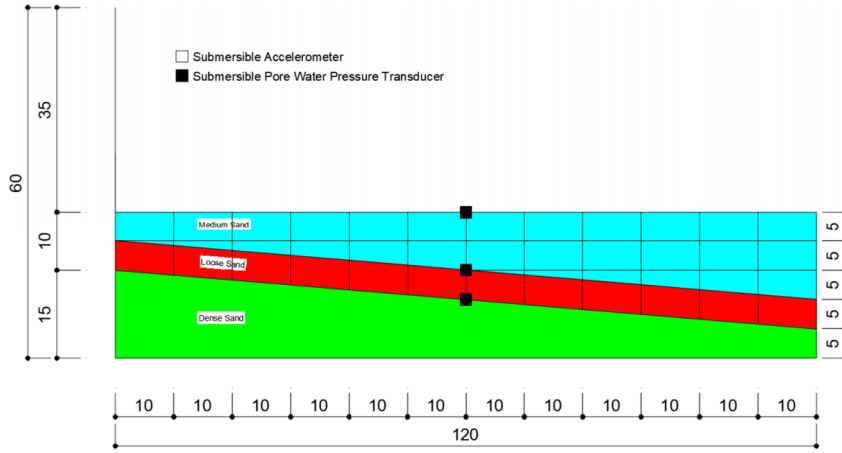


Fig. 1. Simulated tank of liquefaction. Three (3) layers with certain gradient compositions were made to present geological conditions.

Soil models are approached with the UBC3D-PLM MODEL. In this model, all parameters are correlated with N-SPT corrected. In this study, parameters are used as seen in Table 1.

Table 1. Soil parameter for simulation.

| Density | Type | (N ₁) ₆₀ | γ_{unsat} (kN/m ³) | γ_{sat} (kN/m ³) | K^e_B | K^e_G | K^P_G |
|---------|---------------|---------------------------------|---------------------------------------|-------------------------------------|---------|---------|---------|
| Loose | Undrained (A) | 5 | 17 | 20 | 519.46 | 742.09 | 155.66 |
| Medium | Undrained (A) | 10 | 18.5 | 21.5 | 654.47 | 934.95 | 380.49 |
| Dense | Undrained (A) | 30 | 21 | 22.5 | 943.87 | 1348.39 | 3740.64 |

| Density | Type | m_e | n_e | n_p | c | ϕ_{ev} | ϕ_p | R_f |
|---------|---------------|-------|-------|-------|-----|-------------|----------|-------|
| Loose | Undrained (A) | 0.5 | 0.5 | 0.4 | 0 | 34 | 34 | 0.864 |
| Medium | Undrained (A) | 0.5 | 0.5 | 0.4 | 0 | 36 | 37 | 0.779 |
| Dense | Undrained (A) | 0.5 | 0.5 | 0.4 | 0 | 35 | 41 | 0.660 |

2.2 Input Ground Motion

Dynamic simulation in this study employing ground motion downloaded from the PEER Database. The acceleration value ranges from 0.3 – 0.6 g to observe the sensitivity area liquefied. Further description of ground motion can be seen in Table 2.

Table 2. List of Ground Motion used for this simulation.

| RSN | Earthquake Name | Station Name | Year | M_w | PGA (g) | Duration (s) |
|------------|------------------------|-------------------------------|-------------|----------------------|----------------|---------------------|
| 1642 | Sierra Madre | Cogswell Dam – Right Abutment | 1991 | 5.61 | 0.302 | 40 |
| 3473 | Chi – Chi, Taiwan – 06 | TCU078 | 1999 | 6.3 | 0.387 | 75 |
| 753 | Loma Prieta | Corralitos | 1989 | 6.93 | 0.645 | 40 |

3 Results and Discussion

The simulation shows that deformation increases with the bigger magnitude and PGA. On the other hand, the duration is not too sensitive to the results. For RSN 1642, 3473, and 753, the deformations have the same pattern: they increase on the right side, where the medium sand is thicker and also points towards the foot of the slope. The deformation pattern can be seen in Fig. 2.

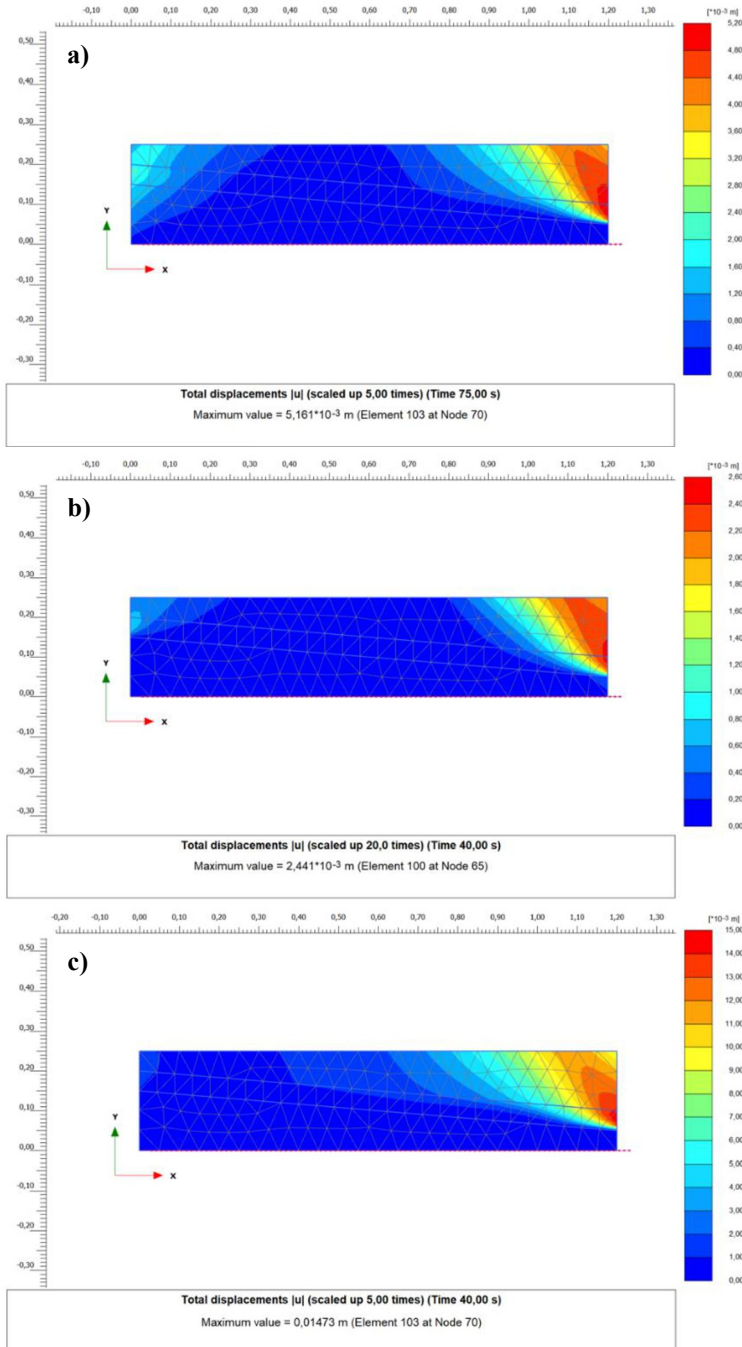


Fig. 2. Deformation resulted by various ground motion. RS 1642 (a), RS 3473 (b), RS 753. Maximum deformation can be observed in each scenario. Biggest deformation happened in RS 753 which is up to 1.473 cm, on other hand the smallest one in RS 1642, i.e. 5.151 mm.

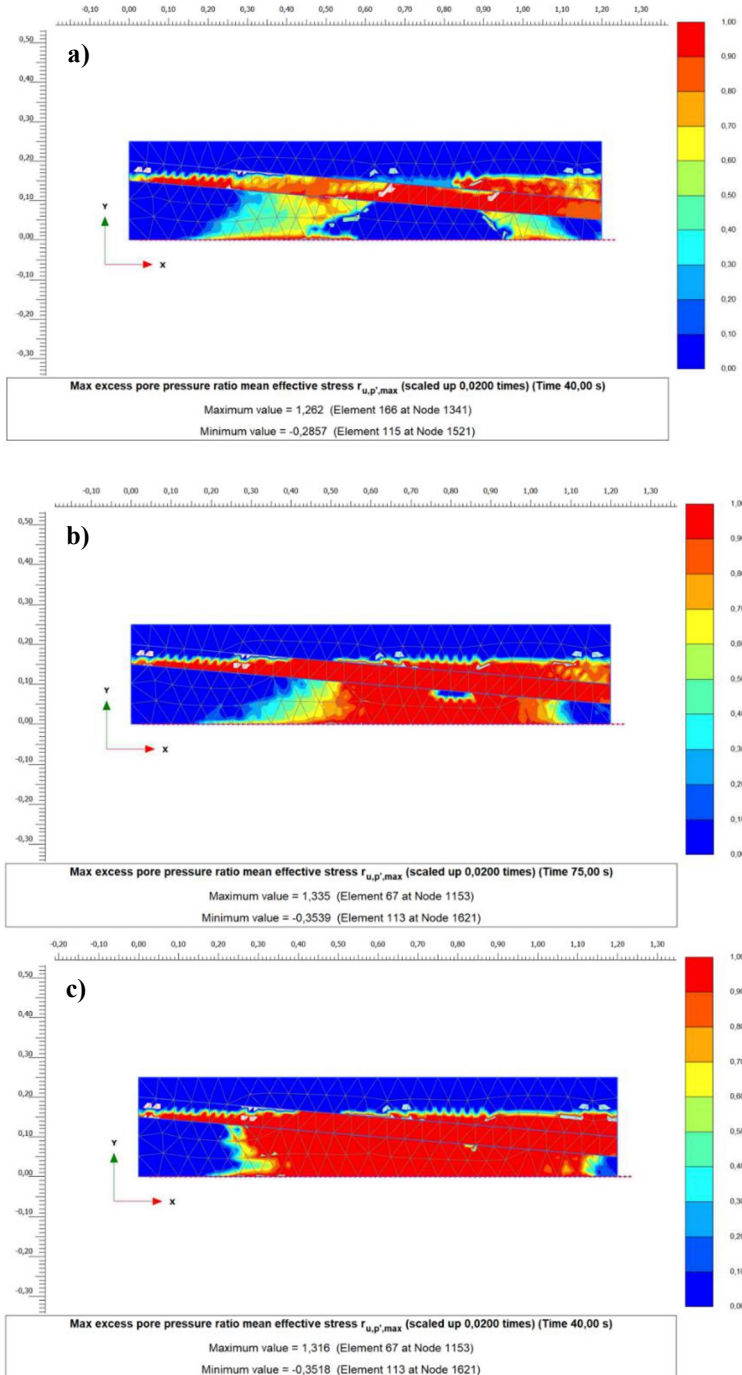


Fig. 3. Max excess pore pressure mean effective stress (r_u) resulted by various ground motion. RS 1642 (a), RS 3473 (b), RS 753. Maximum ratio happened in RS 3473 but biggest area happened in RS 753.

For maximum excess pore pressure, the mean effective stress parameter (r_u) depends very much on the duration of ground motion rather than magnitude. However, the area liquefied is still predominantly caused by the magnitude and PGA value.

4 Conclusion

A numerical simulation study of liquefaction as a comparison to laboratory results has been carried out. Based on this study, liquefaction events can be manifested in the form of deformation and liquified areas. The greater the acceleration applied to the model, the greater the deformation (i.e. 1.473 cm for an acceleration of 0.645g). Deformation will be greater if there is a loose layer at a greater depth. Indications of liquefaction can be seen in the r_u parameter. Areas that have the parameter $r_u > 1$ will experience liquefaction. The greater the acceleration and time of the earthquake, the greater the liquefaction area.

References

1. A. Socquet, J. Hollingsworth, E. Pathier, and M. Bouchon, *Nature Geoscience* **12**, 192 (2019)
2. H. B. Mason, A. P. Gallant, D. Hutabarat, J. Montgomery, A. N. Reed, J. Wartman, M. Irsyam, W. Prakoso, D. Djarwadi, and D. Harnanto, (2021)
3. T. C. Upomo, M. Chang, R. Kusumawardani, G. A. Prayitno, R.-C. Huang, and M. H. Fansuri, in (IOP Publishing, 2023), p. 012007
4. S. Valkaniotis, A. Ganas, V. Tsironi, and A. Barberopoulou, Zenodo: Genève, Switzerland (2018)
5. A. Jalil, T. F. Fathani, I. Satyarno, and W. Wilopo, *Geoenvironmental Disasters* **8**, 21 (2021)
6. A. Tohari, D. D. Wardhana, M. Hanif, and K. Koizumi, in (EDP Sciences, 2021), p. 03002
7. W. Araujo and C. Ledezma, *Applied Sciences* **10**, 6503 (2020)
8. K. Ishihara and M. Takeuchi, (1991)
9. Y. Sasaki, H. Matsumoto, K. Tokida, and S. Saya, (1991)
10. R. M. Varghese and G. Madhavi Latha, *Natural Hazards* **73**, 1337 (2014)
11. K. Tokida, H. Matsumoto, T. Azuma, and I. Towhata, *WIT Transactions on The Built Environment* **3**, (1970)
12. H. Toyota, I. Towhata, S.-I. Imamura, and K.-I. Kudo, *Soils and Foundations* **44**, 67 (2004)
13. A. J. Rivera, C. G. Olgun, T. L. Brandon, and F. Masse, in *IFCEE 2015* (2015), pp. 2214–2224
14. X. Yang, Y. Zhang, and Z. Li, *Minerals* **10**, 218 (2020)
15. R. Brinkgreve, S. Kumarswamy, W. Swolfs, D. Waterman, A. Chesaru, and P. Bonnier, PLAXIS Bv, the Netherlands (2016)